THE JOURNAL OF BIOLOGICAL CHEMISTRY

Vol. 268, No. 23, Issue of August 15, pp. 17286–17299, 1993
Printed in U.S.A.

Self-assembly and Calcium-binding Sites in Laminin

A THREE-ARM INTERACTION MODEL*

(Received for publication, March 4, 1993, and in revised form, April 21, 1993)

Peter D. Yurchenco‡ and Yi-Shan Cheng

From the Department of Pathology, the Robert Wood Johnson Medical School, Piscataway, New Jersey 08854

Laminin, a four-arm glycoprotein, polymerizes *in vitro* into networks similar to those found in basement membranes. We have dissected this calcium-dependent assembly by analyzing proteolytic fragment binding using equilibrium gel filtration, ultracentrifugation, and electron microscopy. The cathepsin G fragment C1–4 (three short arms) was found to aggregate with a critical concentration similar to that for laminin. Like laminin polymerization, this assembly was inhibited by the smaller elastase short arm fragments E4 (B1 domains VI and V) and E1′ (A-B2 short arm complex). Fragment E4 bound directly to E1′ in a calcium-dependent manner (K_D = 1.4 μM). In contrast, homologous self-interactions of short arm fragments and all interactions of long arm fragments were considerably weaker or nonexistent. While electron micrographs of E1′ or E4 alone contained mostly monomers, those of E1′/E4 mixtures contained dimers and oligomers with E1′ dimers connected to each other through their A and B2 arms, often with visible E4 molecules at their junctions. $^{45}Ca^{2+}$ bound principally to fragment E1′ with localization to the end of the B2 chain. These data support a model in which polymerization requires the interaction of all three ligands, one from each short arm, with calcium activating assembly by binding to the B2 short arm.

Laminin plays both architectural and cell-interactive roles in basement membranes. In its "classical" form, the glycoprotein monomer is composed of three polypeptide chains (A, B1, and B2) that join through disulfide-stabilized coiled-coil interactions to form a cruciform structure with three short arms and one long arm (reviewed by Beck *et al.* (1990)). In the Engelbreth-Holm-Swarm (EHS)[1] tumor basement membrane, laminin is present in roughly equimolar (~13 μM) concentrations with type IV collagen (Fujiwara *et al.*, 1984; Yurchenco and Schittny, 1990), and typically one arm (B2) is tightly associated with a fourth polypeptide chain, entactin/nidogen (Paulsson *et al.*, 1987; Gerl *et al.*, 1991).

Laminin undergoes a thermally reversible polymerization in the presence of calcium in which the overall assembly follows nucleation-propagation thermodynamic behavior with a typical critical concentration of 0.1 μM (Yurchenco *et al.*, 1985). Electron micrographs suggested that peripheral short and long arm interactions were involved in this assembly, and, given the cooperativity of the interactions, the individual protein-ligand interactions crucial for polymerization were expected to be ones of low affinity (Yurchenco *et al.*, 1985; Schittny and Yurchenco, 1990). Calcium has been found to play an important role in laminin and laminin polymer structure and function. It was found that calcium was the most effective divalent cation in mediating polymerization, that calcium bound in molar excess to laminin/nidogen (Paulsson, 1988), that calcium appeared to be required for a functional laminin conformation (Paulsson *et al.*, 1988), and that EDTA could be used to selectively extract laminin complexed to entactin from the EHS tumor (Paulsson *et al.*, 1987) as well as a laminin variant found in heart (Paulsson and Saladin, 1989) and placenta (Engvall *et al.*, 1992). The short arm elastase fragment E4 was furthermore found to bind to intact laminin in a calcium-dependent manner by the method of affinity retardation chromatography (Schittny and Yurchenco, 1990).

The same polymer observed *in vitro* has been identified in collagen-free basement membranes of the embryonic carcinoma cells and in the collagen-rich basement membrane of the EHS tumor (Yurchenco *et al.*, 1992). Short arm proteolytic fragments that inhibit polymerization (Schittny and Yurchenco, 1990) were found to selectively solubilize laminin from these two basement membranes (Yurchenco *et al.*, 1992). In the EHS basement membrane, two major networks were identified. Laminin formed one network, and type IV collagen formed the other. Twenty percent of the laminin molecules were also immobilized in the basement membrane by noncovalent cross-links to the type IV collagen network. One of the major components likely to mediate this cross-linking is entactin/nidogen (Aumailley *et al.*, 1989; Fox *et al.*, 1991), and there may be other components as well (Yurchenco *et al.*, 1992).

In this study, we have evaluated the polymerization of a fragment carrying the three short arms. We have also extensively dissected and quantitated the inter-laminin and calcium-laminin binding interactions of a variety of different defined fragments representing nearly all the domains of laminin using equilibrium gel filtration, equilibrium zonal ultracentrifugation, and electron microscopy of fragment mixtures. From the data we have developed a three-arm interaction hypothesis of laminin assembly.

MATERIALS AND METHODS

Preparation and Labeling of Laminin and Its Fragments

Purification steps were carried out at 0–5 °C. Laminin and laminin/entactin were isolated from lathyritic EHS tumors based on the EDTA extraction method of Paulsson *et al.* (1987) and purified as

* This work was supported by Grant RO1-DK36425 from the National Institutes of Health. The costs of publication of this article were defrayed in part by the payment of page charges. This article must therefore be hereby marked "*advertisement*" in accordance with 18 U.S.C. Section 1734 solely to indicate this fact.

‡ To whom correspondence should be addressed: Dept. of Pathology, Robert Wood Johnson Medical School, 675 Hoes Lane, Piscataway, NJ 08854. Tel.: 908-235-4674; Fax: 908-235-4825.

[1] The abbreviations used are: EHS, Engelbreth-Holm-Swarm; PAGE, polyacrylamide gel electrophoresis; TBS, Tris-buffered saline; G domain, laminin long arm globular domain.

described (Yurchenco *et al.*, 1992). Fragments (see Fig. 1) (Ott *et al.*, 1982; Fujiwara *et al.*, 1988; Mann *et al.*, 1988; Paulsson, 1988; Deutzmann *et al.*, 1988; Bruch *et al.*, 1989; Schittny and Yurchenco, 1990) were generated by digestion with elastase, pepsin, and cathepsin G. Elastase fragment E3 consists of the distal two subdomains of the long arm globule, and fragment E8 consists of the distal moiety of the long arm rod domain and adjacent proximal globular subdomains (Deutzmann *et al.*, 1988). Fragment E4 consists of NH_2-terminal B1 chain short arm domains VI and V (Fujiwara *et al.*, 1988), and fragment E10 (25 kDa) corresponds to the inner globule of the B1 chain, *i.e.* domain IV (Mann *et al.*, 1988). Fragment E10′ has a molecular mass of 20 kDa by SDS-PAGE. It is similar to fragment E10 (25 kDa) in that we found it specifically reacted in immunoblots with rabbit polyclonal antiserum specific for mouse recombinant B1 domain IV (*Bst*XI-*Sma*I cDNA fragment inserted in the pET3b vector) produced in isopropyl-1-thio-β-D-galactopyranoside-induced *Escherichia coli* strain BL21(DE3) following the method of Studier *et al.* (1990).[2] Cathepsin G fragment C1–4 is a large complex consisting of all three short arms with portions of entactin/nidogen bound to the B2 short arm (Bruch *et al.*, 1989). The preparations are summarized as follows. Elastase fragments E1′, E4, E8, and E3 of laminin were generated by digestion with elastase at a 1:200 or 1:250 enzyme/substrate ratio (25 °C, 23 h) followed by gel filtration (Sepharose CL-6B) and DEAE-Sephacel ion-exchange chromatography as described (Schittny and Yurchenco, 1990; Yurchenco *et al.*, 1992), except that a narrow portion of the DEAE peak of E1′ was used for higher purity. Fragment P1′ was prepared from a pepsin digest of laminin by agarose 1.5m gel filtration (Calbiochem) in 1 M calcium chloride as described (Schittny and Yurchenco, 1990). Fragment E1 was isolated following a more extensive digestion with elastase (1:100 enzyme/substrate ratio, 37 °C, 47 h) in the same manner as E1′. Fragment C1–4 was generated by incubation of laminin with cathepsin G (Calbiochem) in TBS (50 mM Tris-HCl, 90 mM NaCl, pH 7.4) containing 1 mM calcium at an enzyme/substrate mass ratio of 1:300 for 5 h at 37 °C (Bruch *et al.*, 1989). The C1–4 precipitate was then pelleted by centrifugation, resuspended in TBS containing 10 mM EDTA, and dissolved by incubation overnight on ice. A sample of fragment E10 (Mann *et al.*, 1988) was a kind gift of Dr. Rupert Timpl (Max-Planck-Institute for Biochemistry, Martinsried, Germany). A related fragment we call E10′ was prepared from elastase digests (E1′ conditions) as follows. The Sepharose CL-6B gel filtration peak fractions containing E3 were bound to a DEAE-5PW ion-exchange column in 50 mM Tris-HCl, pH 8.5, and subjected to a linear 0–1 M NaCl gradient (E10′ eluted at an applied NaCl concentration of 0.2 M). The pooled protein was then bound to a phenyl-Superose column (5 cm, inner diameter, × 0.5 cm, Toso-Haas) in 1.5 M ammonium sulfate in 10 mM sodium phosphate, 127 mM NaCl, pH 7.4, and eluted as the first major peak with a decreasing linear gradient of ammonium sulfate. Laminin and laminin fragments were stored in TBS with 0.1 mM EDTA.

Laminin, laminin/entactin, and fragments E1′, E1, P1′, E3, and E4 were radioiodinated with $Na^{125}I$ by a lactoperoxidase method and purified by chromatography on a Sepharose CL-6B column as described (Schittny and Yurchenco, 1990). Fragment C1–4 was radioiodinated with Bolten-Hunter reagent (Du Pont-New England Nuclear) by incubating protein (60–70 μg of protein in 30 μl) in 0.2 M sodium borate HCl, pH 8.2, with the radiolabel for several hours on ice followed by Sepharose CL-6B gel filtration.

Antibodies and Immunoblotting

Polyclonal antibody specific for laminin A chain domain VI was a kind gift of Dr. Amy Skubitz (University of Minnesota). Rabbit antiserum to a synthetic peptide consisting of residues 42–63 (RPVRHAQCRVCDGNSTNPREHR) was purified by ammonium sulfate precipitation and DEAE column chromatography. In electrophoretically transferred immunoblots (Towbin *et al.*, 1979), the antibody reacted with E1′, but not with elastase fragments E3, E8, and E4, a chymotryptic 440-kDa laminin fragment (Palm *et al.*, 1985), or intact fibronectin.

Protein Determinations, SDS-Polyacrylamide Gel Electrophoresis, and NH_2-terminal Sequencing

Protein in solution was determined either by absorbance at 280 nm (for protein cleared of turbid material) or colorimetrically (Schittny and Yurchenco, 1990). The absorbance (280 nm) extinction coefficients used were $\epsilon = 750\ g^{-1}\ cm^2$ for laminin (protein M_r = 710,000) and laminin/entactin (protein M_r = 835,000; total $M_r \cong$ 1,000,000) (Yurchenco *et al.*, 1990); $\epsilon = 889\ g^{-1}\ cm^2$ for E1′ (M_r = 450,000) (Paulsson, 1988), E1 (M_r = 375,000), and P1′ (M_r = 350,000); $\epsilon = 933\ g^{-1}\ cm^2$ for E4 (M_r = 75,000); $\epsilon = 341\ g^{-1}\ cm^2$ for E8 (protein M_r = 138,000; total M_r = 220,000); and $\epsilon = 895\ g^{-1}\ cm^2$ for E3 (M_r = 50,000). SDS-PAGE was carried out on 3.5–12% linear gradient gels (Laemmli, 1970) as described (Yurchenco *et al.*, 1990) and stained with Coomassie Brilliant Blue R-250. Molecular mass standards used were entactin/nidogen (150 kDa), β-galactosidase (116 kDa), phosphorylase *b* (97.4 kDa), bovine serum albumin (66.2 kDa), ovalbumin (42.7 kDa), and carbonic anhydrase (31 kDa). For sequencing, proteins were separated by SDS-PAGE and electrophoretically transferred (Towbin *et al.*, 1979) onto 0.45-μm polyvinylidene difluoride membranes (Immobilon-P, Millipore). The membrane was then lightly stained with Coomassie Blue, destained, and dried. The stained band of interest was cut out, and the NH_2-terminal sequence was determined by the W. M. Keck Foundation Biotechnology Resource Laboratory at Yale University (New Haven, CT).

Sedimentation Assay for Polymerization

Direct Assay—Laminin samples (0.5 ml) were incubated in TBS containing 1 mM $CaCl_2$ at 35 °C for 2 h in 1.5-ml Eppendorf tubes and then were centrifuged at 10,500 rpm (16,000 × *g*) in a microcentrifuge. The laminin concentration in the supernatant was determined at the beginning of the incubation and following centrifugation by measuring the absorbance at 280 nm as previously described (Yurchenco *et al.*, 1990). The fraction of polymer was calculated by subtracting the supernatant concentration (following centrifugation) from the total laminin concentration.

Inhibition Assay—Samples with constant ^{125}I-laminin (0.25 mg/ml, 35,000–50,000 cpm/mg) or ^{125}I-fragment C1–4 but with variable concentrations of unlabeled ligand were incubated under the above conditions with inhibition determined as described (Yurchenco *et al.*, 1992).

Equilibrium Gel Filtration

To measure low affinity (and hence readily reversible interactions) between pairs of laminin fragments under solution conditions, the method of equilibrium gel filtration (Hummel and Dryer, 1962) as modified for radiolabeled macromolecules (Horwitz *et al.*, 1985) was employed. Sepharose CL-2B, Sepharose CL-6B, and Sephadex G-150 (this gel used only for evaluation of E10′ self-interactions) beads (Pharmacia LKB Biotechnology Inc.) equilibrated in TBS were packed into 50-cm-long columns (3-mm internal diameter) surrounded by a water jacket whose temperature was maintained by a circulating refrigerator/heater water bath. The column was permeated with buffer alone in the presence of 0.1 mg/ml bovine serum albumin (Sigma) as carrier protein (the bovine serum albumin prevented loss of protein to the column without affecting the nonbinding K_{av}) or with a protein P at a variety of constant concentrations in TBS containing 1 mM $CaCl_2$ (TBS/Ca) or 5 mM EDTA (TBS/EDTA). The radioiodinated ligand L was then applied to the column as a 60-μl aliquot, and 3-drop (75 μl) fractions were collected. An internal [^{35}S]sodium sulfate standard was added to correct for small variations in volumes. The position of phenol red was defined as a marker for the included volume (V_t). The first blue dextran 5000 (Pharmacia) peak was used to determine the void volume (V_0) in the Sepharose CL-6B and Sephadex G-150 columns, and a large E1′-soluble aggregate produced by oxidation was used to define V_0 in the Sepharose CL-2B gel filtration column.

The principle of the method is as follows. Component P is allowed to permeate a gel filtration column so that a radiolabeled ligand L, applied as a narrow band, will remain in the presence of constant P throughout its passage through the column. The ligand L will elute from the column as a larger species at the K_{av} of the complex if strongly associated with P. If the equilibrium is such that it only spends part of the time bound to P, then it should elute between the elution volume of the complex and L weighted according to the fraction of time the ligand spends in the bound and free states. This situation is analogous to that described for heparin binding to protein using the method of affinity coelectrophoresis (Lee and Lander, 1991; Lim *et al.*, 1991). In both systems, the dissociation equilibrium constant can be determined by Scatchard analysis (Cantor and Shimmel, 1980) or by nonlinear regression analysis of the migration behavior of the ligand at different concentrations of an interacting permeating protein. We can define a relative unitless elution coefficient r =

[2] J. J. O'Rear and P. D. Yurchenco, unpublished data.

$(K_o - K_x)/K_o$, where K_o corresponds to the nonbinding K_{av} of radiolabeled ligand L and K_x corresponds to the K_{av} of L at a constant free molar permeating protein concentration, [P]. Since r at a given protein concentration should be proportional to the amount of ligand bound, then for a single class of interaction, a plot of $r/[P]$ *versus* r will give a straight line with a slope of $-1/K_D$, a y intercept of r_{sat}/K_D, and an x axis intercept of r_{sat}. The term r_{sat} is the value of the elution coefficient under saturating conditions at infinitely high concentrations of protein P. The K_{av} at saturation ($K_{sat} = K_o(1 - r_{sat})$) in turn can provide a molecular mass estimate for the complex at saturation if the column is calibrated. Since the free concentration of P cannot be measured directly, the concentration of L is maintained much less than P (as a trace radioligand), permitting the free concentration to be very close to the total concentration of P. The dissociation constant can also be determined by nonlinear regression analysis (preferred method) according to the algorithm of Marquardt-Levenberg (provided in SigmaPlot version 5.0, Jandel Scientific, San Rafael, CA) in which the function $(r_{sat}[P])/(K_D + [P])$ is fitted to the observed r values. Putative binding combinations can also be evaluated with single determinations (Horwitz *et al.*, 1985) if K_{sat} is known or can be predicted. Here the dissociation constant is estimated from the derivation $K_D = ([P](K_x - K_{sat}))/(K_o - K_x)$. Finally, the sensitivity of an equilibrium gel filtration determination is dependent upon the magnitudes of [P] and $(K_o - K_{sat})$. The latter parameter is expected to be greater for simple binding if the smaller of two interacting proteins is used as the labeled ligand (*i.e.* when K_{av} of L > K_{av} of P).

Equilibrium Zonal Ultracentrifugation

A change in zonal sucrose velocity sedimentation behavior of a labeled protein in the presence of a constant level of binding species can also be used to detect low affinity binding. A restriction of this method is that the labeled species must sediment faster than the permeating species. This method was used to evaluate intact laminin interactions because, in contrast to laminin fragments, we found that intact laminin tended to aggregate on or in the Sepharose gel at 37 °C either in binding buffer or EDTA buffer. The centrifugation procedure was modified from that used previously (Yurchenco *et al.*, 1990) as follows. Radioiodinated laminin (0.2 ml) was applied to the top of 12.6-ml 5–20% (w/v) linear sucrose gradients in TBS/Ca or TBS/EDTA alone or containing constant protein. The tubes were centrifuged in a Beckman SW 40-Ti rotor at 40,000 rpm for 8 h at 37 °C. Fractions (0.2 ml) were collected with a Buchler Auto Densi-Flow II fractionation device, collecting from top to bottom. Cytochrome *c*, aldolase, and catalase standards (1.8, 7.35, and 11.3 S, respectively) were sedimented in parallel tubes.

Calcium Binding

Dot Blot Method—Water, treated by filtration through Chelex beads (Bio-Rad), was used in the buffers of this procedure. A nitrocellulose membrane (0.2 μm, Schleicher & Schuell), washed in 60 mM KCl, 5 mM $MgCl_2$, 10 mM imidazole HCl, pH 7.0 (calcium binding buffer), was fitted to a 96-well vacuum manifold (Bethesda Research Laboratories). Aliquots (50 μl) of protein samples, in 2-fold serial dilutions, were applied to the wells and washed with 0.1 ml of buffer, and the buffer was removed by vacuum. The sheet was then incubated with $^{45}CaCl_2$ (7–17 mCi/mg of calcium; ICN Biomedicals, Irvine, CA) diluted to 1 μCi/ml (~1–2 μM) in calcium binding buffer at room temperature for 10 min. After washing the membrane with water, it was dried, cut up, and dissolved in 5 ml of Filtron-X (National Diagnostics, Inc). Radioactivity was determined using a Beckman LS-6000 liquid scintillation counter equipped with automatic color quenching correction and chemiluminescence detector.

SDS-PAGE/Electrophoretic Transfer Method—The method of Maruyama *et al.* (1984) was used. Briefly, approximately equimolar amounts of laminin, entactin, and laminin fragments were electrophoresed on 3.5–12% gradient acrylamide gels (SDS-PAGE) and then transferred from the gels onto 0.2-μm nitrocellulose sheets in 25 mM Tris, 192 mM glycine, 20% (v/v) methanol buffer, pH 8.3, at 10–11 V-h/cm by the Western blot method of Towbin *et al.* (1979). The nitrocellulose membrane was then incubated with $^{45}CaCl_2$ (1 μCi/ml) for 10 min as described above. After washing and drying, autoradiographs were prepared by sandwiching Kodak X-Omat R film with plastic wrap-covered membranes between fluorescent intensifying screens and exposing at −80 °C for 24–48 h.

Platinum/Carbon Replication and Electron Microscopy

Replicas of proteins for electron microscopy were prepared by platinum/carbon rotary shadowing (8° angle) as described (Yurchenco *et al.*, 1992). Preparations of incubated proteins were sprayed onto mica immediately upon the addition of glycerol. Metal replication was accomplished with a BAF500K system (Bal-tec, Middlebury, CT), and micrographs were prepared contrast-reversed to enhance image perception. Contour length measurements were made with a digitizing pad and Lex 90 display monitor (Lexidata, Billerica, MA) interfaced with a DEC Microvax II computer (Digital Equipment Corp., Merrimack, NH) following digitalization of the electron microscopy plates (magnification × 45,000) with a System P-1000 digitizer (Optronics Instruments, Chelmsford, MA) using a 50-μm raster size.

RESULTS

Laminin Fragments—Laminin fragments (Fig. 1) were used to localize binding interactions. Fragment E4 has previously been shown to inhibit laminin polymerization and to bind to intact laminin (Schittny and Yurchenco, 1990), and fragment C1–4, which consists of all three short arms, was found to selectively precipitate during its preparation, implicating an important role for this laminin moiety in polymerization (Bruch *et al.*, 1989). There are also three Y-shaped short arm complexes contained within the regions of laminin represented by C1–4. These complexes each contain the A and B2 arms as well as the inner rod-like domain (III), or "stub", of the B1 chain (Fig. 1, *inset*). The three fragments are E1′

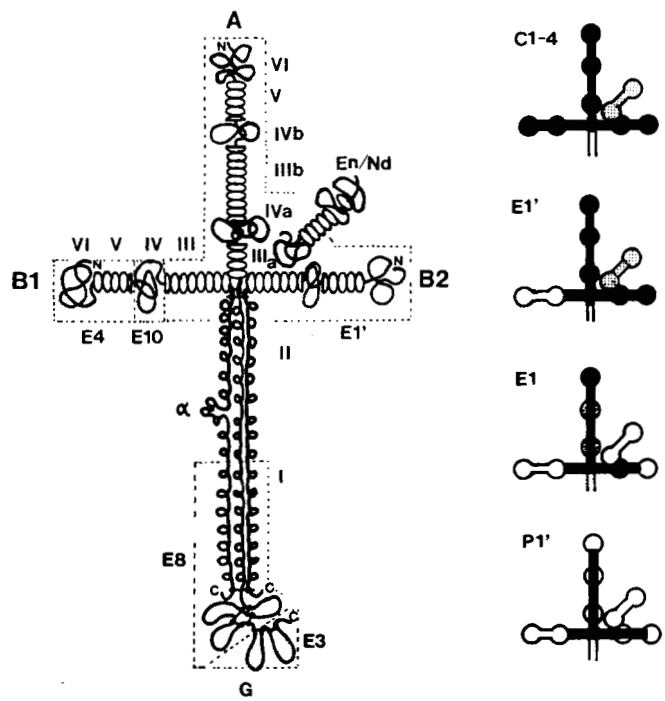

FIG. 1. **Diagram of laminin and its fragments.** EHS laminin contains B1, A, and B2 chains joined together to form a four-arm structure. Entactin/nidogen (*En/Nd*) is commonly found bound to the B2 short arm. Elastase (*E*), cathepsin G (*C*), and pepsin (*P*) have been used to generate a series of fragments corresponding to different regions of laminin. These are E4 (B1 domains VI and V), E1′ (A-B2 chain short arm complex containing all globular domains, B1 domain III, and fragmented entactin), P1′ (A-B2 chain short arm complex lacking globular domains and entactin), E1 (intermediate in size between E1′ and P1′ and lacking the B2 outer globule), C1–4 (short arm complex containing all three short arms with their globules), E8 (long arm fragments containing distal part of the long arm and G subdomains 1–3), and E3 (distal long arm globule with G subdomains 4 and 5). Some degree of structural heterogeneity is found in the A-B2 short arm complexes (*shaded* regions in *insets* represent domains present in many, but not all molecules).

(Paulsson *et al.*, 1988), E1 (Ott *et al.*, 1982), and P1′ (Schittny and Yurchenco, 1990). To further define differences between these complexes, we compared the fragments by SDS-PAGE, electron microscopy, and morphometry and further characterized P1′ by NH_2-terminal sequence analysis (Fig. 2 and Table I). All three fragments possessed very similar contour arm lengths (Table I), which, for the A and B2 chains, were similar to the arm lengths measured for intact laminin. Fragments E1′, E1, and P1′ each were different with respect to the domains present (Table I) and with respect to binding activity (described below). It is important to note that in fragment E1′ (the largest of the three fragments), the A and B2 short arm globules were all present (Fig. 2*d*). It was also found that fragmented entactin structures (dumbbell-shaped or just a globule) were observed to be in association with one out of four B2 short arms. Fragment E1, obtained by further digestion, was a little smaller than E1′. It significantly possessed the peripheral globule (domain VI) of the A short arm, but lacked the peripheral globule of the B2 short arm (Fig. 2*e*). It also lacked entactin domains, and some molecules lacked inner (in contrast to peripheral) A chain globules. Fragment P1′, which can be generated from intact laminin or from E1′, was the smallest of the three complexes and lacked all recognizable globular domains (Fig. 2*g*).

The fragments were also compared by SDS-PAGE (Fig. 2, *a–c*). Fragments C1–4, E1′, E1, and P1′ all migrated as large species ranging in size from C1–4 (largest) to P1′ (smallest). Other smaller and less prominent bands were present as well. In the case of E1′, the ~90-kDa band has been found to be a fragment of entactin/nidogen (Mann *et al.*, 1988), while the ~33-kDa band is an NH_2-terminal domain of laminin, identified by its reaction with laminin A chain domain VI antibody (immunoblot not shown). Under reducing conditions, the A and B chain components separated. In the case of E1 and P1′, these chains dissociated into a series of smaller fragments, and therefore, they are held together as a single species by intrachain disulfide bonds. The three main reduced bands of P1′ (65, 35, and 32 kDa) were subjected to NH_2-terminal analysis and found to have the following sequences, respectively: LXQTGLAXE (starting at residue 745 of the B1 chain), ISVGGMXIX (starting at residue 247 of the A chain), and FAVGG (starting at residue 245 of the B2 chain). These residues are found very near the junction of the inner globule (domain IV) and rod (domain III) of the B1 chain and near the junction of the outer globules (domain VI) and outer rods (domain V) of the A and B2 chains (Sasaki *et al.*, 1987, 1988; Sasaki and Yamada, 1987) and thus are in agreement with the morphological data. Fragments E1′ and E1, but not P1′, were found to react with rabbit anti-A chain domain VI antibody by Western blot analysis (immunoblots not shown), consistent with the presence of the A short arm globules in E1′ and E1, but not in P1′, by electron microscopy. Our interpretations of the regions of laminin represented by these fragments are shown in Fig. 1.

Polymerization of Fragment C1–4—Soluble fragment C1–4 formed sedimentable aggregates when incubated in TBS/Ca at 37 °C. The concentration dependence of the reaction (Fig. 3*a*) was linear over the range studied (slope = 0.93), with an x intercept of 30 μg/ml (0.06 μM) interpreted as corresponding to the critical concentration of polymerization. This compares to a critical concentration of 0.1 μM typically found for intact laminin (although some preparations have been as low as 0.05 μM) (Yurchenco *et al.*, 1985, 1990, 1992). Fragments E1′ and E4, but not P1′ (to any significant degree), inhibited the aggregation of C1–4 (Fig. 3*b*). These data are in agreement with those observed with intact laminin. Fragment C1–4 was the only fragment of laminin that polymerized. Unfractionated elastase digest mixtures inhibited polymerization, and all purified fragments either inhibited polymerization (E1′, E1, and E4) or failed to effectively inhibit polymerization (E10′, E8, and E3). Thus, we concluded that the principal polymerization activity of laminin is localized in the short arms of laminin and, in agreement with earlier conclusions (Bruch *et al.*, 1989), that the long arm and its globule are not required.

Equilibrium Gel Filtration of E4 + E1′—Our previous finding that fragments E4 and E1′ inhibit laminin polymerization (Schittny and Yurchenco, 1990), shown now also for C1–4 aggregation (Fig. 3), suggested there is an interaction between these two fragments. This was tested by the sensitive method of equilibrium gel filtration in which binding was carried out under solution conditions for both species (Fig. 4). Fragment E4 alone eluted from a Sepharose CL-2B column with a nonbinding K_{av} of 0.75 both in TBS/Ca and TBS/EDTA. In calcium-containing buffer and at 37 °C in the presence of constant (2 mg/ml) E1′, fragment E4 eluted as a considerably larger species with a K_{av} of 0.36 (Fig. 4*A*). The K_{av} was even less than that of E1′ alone (position marked with an *arrow*). At 5 °C, the elution K_{av} increased to 0.65. In EDTA at 37 °C, the elution K_{av} was 0.54, and in EDTA at 5 °C, the elution K_{av} was 0.68. Thus, E4 bound to E1′, and the interaction was strongly facilitated by elevated temperature and moderately facilitated by the presence of calcium. The concentration dependence of this association was examined (Fig. 4*B*). The K_{av} value decreased as a function of increasing the constant column concentration of E1′, and saturation was approached at the higher concentrations. As described under "Materials and Methods," the relationship between elution behavior and E1′ concentration can be used to calculate a dissociation constant as well as to estimate the size of the complex under conditions of saturation binding (Fig. 4*C*). For this determination, the elution coefficient r was plotted against the molar concentration of E1′, and both the direct binding plot and Scatchard transformation (*inset*) are shown. A good curve fit was obtained for a single class of binding with a dissociation constant of 1.4 μM. This number was confirmed by a Scatchard transformation (*inset*). Furthermore, an r_{sat} (value of r at saturation of E4 binding) of 0.69 was determined by nonlinear regression analysis (the Scatchard transformation values were slightly higher), which corresponded to a K_{av} of 0.2. From the column calibration, the $K_{av/sat}$ value corresponded to a molecular weight of $\sim 1.6 \times 10^6$. This is consistent with an average complex (size heterogeneity is assumed) containing three to four E1′ molecules and an equivalent number of E4 molecules. The size of the E1′-E4 complex at saturation indicated that we were not simply looking at a dimerization between two ligands, but rather a more complicated assembly of oligomerization with an apparent overall dissociation constant as determined. This interaction was further evaluated by electron microscopy as described below.

Equilibrium Gel Filtration Analysis of Other Interactions—The question arose as to whether interactions between the short arms were restricted and, in particular, whether the B1 chain fragment E4 bound to itself and whether the A-B2 complex bound to itself. Equilibrium gel filtration (Fig. 5, *a–e*) was used to address these questions. If a single molecular species forms homodimers or larger complexes as a function of increased concentration, then the K_{av} should shift to a lower value, and the dimer saturation condition could be predicted by column calibration (Fig. 5, *f* and *g*). When radiolabeled E1′ was passed down the column in the absence of permeating E1′, it eluted with a nonbinding K_{av} of 0.52

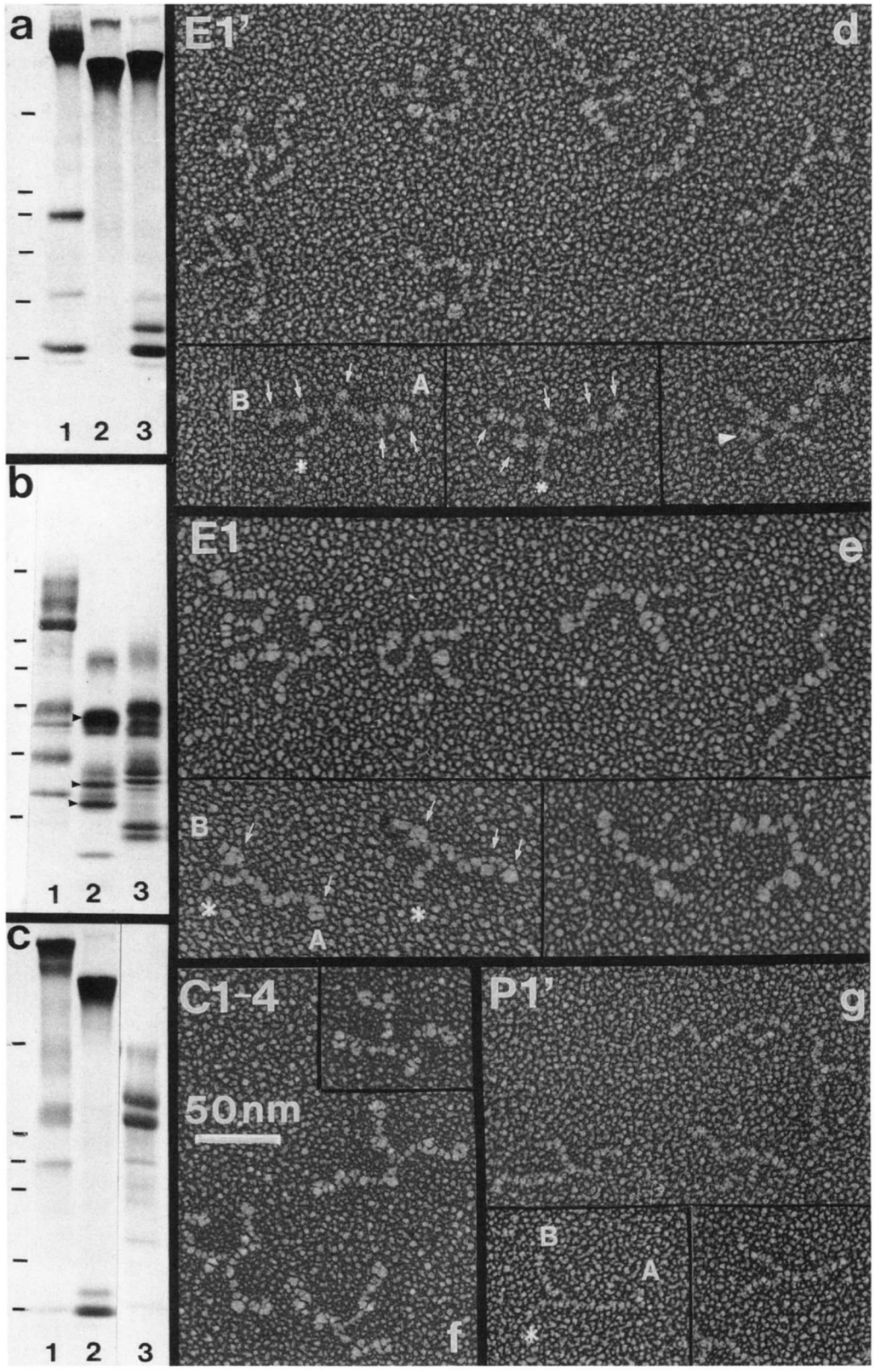

FIG. 2. **Comparison of short arm complexes.** Purified fragments were analyzed by SDS-PAGE (*a–c*) and rotary-shadowed at a low angle with platinum/carbon (*d–g*). Coomassie Blue-stained lanes are as follows. *a*, *lane 1*, elastase fragment E1′ (nonreduced); *lane 2*, pepsin fragment P1′ (nonreduced); *lane 3*, elastase fragment E1 (nonreduced). *b*, *lane 1*, E1′ (reduced); *lane 2*, P1′ (reduced); *lane 3*, E1 (reduced). *c*, *lane 1*, cathepsin G fragment C1–4 (nonreduced); *lane 2*, E1 (nonreduced); *lane 3*, C1–4 (reduced). Molecular mass standards are indicated to the left (200, 116, 97, 66, 43 and 31 kDa). Intramolecular disulfides hold each of the complexes together as single molecular species. *Arrowheads* in *b* (*lane 2*) indicate P1′ bands transferred to a polyvinylidene difluoride membrane for NH_2-terminal sequence analysis (described under "Results"). Electron micrographs of platinum/carbon replicas of E1′ (*d*), E1 (*e*), C1–4 (*f*), and P1′ (*g*) reveal that E1′ has an asymmetrical Y shape with a longer A arm (*A*) carrying terminal and included globules, a shorter B2 arm (*B*) with terminal and included globules, and a short ~25-nm-long rod-like domain (B1 domain III) (*asterisk*). *Arrows* mark examples of globules. About one out of four molecules has a dumbbell-like (*arrowhead*) projection from the B chain, characteristic of entactin/nidogen. Fragment E1 (*e*) has a similar shape, but lacks a

TABLE I

Morphological comparison of Y-shaped laminin short arm complexes

Protein	Contour arm lengths (mean ± S.D.)				Terminal A globule	Terminal B2 globule
	n	Short A	Short B	B1 stub		
		nm	*nm*	*nm*		
Laminin	58	51.5 ± 5.0	37.3 ± 5.0		Yes	Yes
E1′	61	51.8 ± 6.8	34.6 ± 4.7	21.8 ± 4.1	Yes	Yes
E1	75	51.3 ± 5.5	32.3 ± 3.5	25.2 ± 4.0	Yes	No
P1′	62	45.9 ± 6.6	31.6 ± 4.6	20.7 ± 4.6	No	No

(Fig. 5*a*). When chromatographed in the presence of constant E1′ (2 mg/ml, 4.4 μM), the position shifted slightly (and consistently on repeated runs) to a K_{av} of 0.48 compared to a predicted dimer position of 0.33 (*arrow*). A dissociation constant of 17 μM (assuming a dimer) or greater (for any complex larger than a dimer) was estimated from the single elution shift as described under "Materials and Methods." In contrast, E1′ shifted to a substantially lower K_{av} (~0.2) in an equimolar concentration of E4. A shift of this magnitude was expected since this is the reciprocal arrangement of fragments with respect to labeled ligand and constant protein as shown (Fig. 4). The shifted peak showed some heterogeneity with a sharp leading edge and a more trailing tail. A similar binding test was applied to E4 (Fig. 5*b*) using a Sepharose CL-6B column. A high constant concentration of E4 (13.3 μM) was used here to increase sensitivity since the expected shift in K_{av} was not large (predicted E4 dimer K_{sat} of 0.37 is indicated with an *arrow*). No shift was detected from the nonbinding position in TBS/Ca at 37 °C. In this manner, we concluded that while E4 binds to E1′, fragment E1′ interacts very weakly with itself, and E4 does not interact with itself.

Other possible fragment interactions were considered (Fig. 5, *c–e*). E4, as expected (Schittny and Yurchenco, 1990), failed to bind to P1′. The C1–4 data indicated that the long arm was not required for polymerization, but they did not exclude the possibility that the long arm can "decorate" other fragments by independent additional binding interactions. Therefore, the long arm fragments E8 and E3 were evaluated for binding to the other fragments (Fig. 5, *c–e*). Fragment E8 did not interact with any other fragments to any significant degree (Fig. 5 (*c–e*) and Table II). Furthermore, no K_{av} shift, and hence no binding, was detected between fragment E3 and the short arm fragments E1′ and E4. However, a K_{av} shift to 0.57 was observed with E3 ligand at high (13 μM) E3 concentration, and from this, a weak self-interaction K_D of ≥24 μM (assuming formation of a dimer or larger structure) was estimated as described under "Materials and Methods." The interaction was completely blocked in the presence of 1 mM *N*-ethylmaleimide (plot not shown). Given recent observations that E3 can migrate as a disulfide-linked dimer on SDS-PAGE (Yurchenco *et al.*, 1993) and that these dimers are not observed if fragment E3 is first treated with 1 mM *N*-ethylmaleimide, we have concluded that these low affinity interactions are a consequence of highly labile disulfides that can form between two E3 molecules (each E3 possesses 7 cysteines). Since this phenomenon is not observed with intact G domain (Yurchenco *et al.*, 1993), we have further concluded it is unlikely that E3 dimerization plays a biological role in laminin self-interactions. Thus, no secondary long arm interactions have been identified with affinities comparable to those observed between short arm fragments.

A radioiodinated fragment contained in B1 chain domain IV (E10′) was also evaluated for interactions with other fragments as well as with itself (Table II). No significant interactions were detected. The nonbinding K_{av} for E10′ was 0.675, which shifted to 0.66 in the presence of 6 μM E4 and to 0.64 in the presence of 4.4 μM E1′. The corresponding estimates of the K_D were ≥76 and ≥95 μM (assuming a dimer or larger complex) for E4 and E1′, respectively. No K_{av} shift was detected with trace radiolabeled E10′ in the presence of 15 μM unlabeled E10′. A very small shift (estimate ≥120 μM) was detected with 10 μM E3, and no shift was detected with 4.4 μM E8 (Table II).

Equilibrium Zonal Ultracentrifugation of Laminin—Previously, it was found that laminin does not polymerize in the presence of EDTA and that EDTA selectively extracts most laminin-entactin complex from the EHS basement membrane (Yurchenco *et al.*, 1985, 1992). While EDTA inhibits binding between E4 and E1′, the degree of inhibition is less than expected. We therefore evaluated the interaction between intact laminin and E1′ by ultracentrifugation to avoid trapping of laminin (Fig. 6). Laminin was centrifuged at 37 °C in TBS/Ca alone or with E1′ or in TBS/EDTA alone or with E1′. In calcium, laminin sedimented alone at 8.2 ml and in E1′ at 9.2 ml (corresponding to a sedimentation rate shift from 11.25 to 12.4 S), whereas in EDTA, there was almost no detectable shift. Thus, the calcium dependence of the reaction was fully preserved between intact laminin and E1′, but only partially preserved between E4 and E1′. We have found that full calcium dependence is sensitive to denaturation. If intact laminin is treated transiently with 2 M guanidine HCl, it polymerizes with the same critical concentration, but with most of the calcium dependence lost (data not shown). We therefore suspect that proteolytic digestion of laminin leads to a partial loss of the calcium requirement for polymerization through conformational changes, but not loss of a calcium-binding site (see below).

Fragment E1 Interactions—Fragment E1 was found to inhibit the polymerization of both intact laminin and C1–4 (Fig. 3). However, unlike that observed with E1′, we could not detect any K_{av} shift between E1 and E4 by equilibrium gel filtration (Fig. 5*c*). We considered the possibility that E1, which lacks an B2 outer globule, also lacks one out of two (or possibly more) short arm binding sites found in the larger E1′ fragment. In particular, this suggested a cooperative model of assembly in which any fragment containing a single interacting ligand would be capable of inhibiting polymerization, but that only a combination of all reactive ligands would produce significant measurable binding and that fewer ligands would lead to extremely low affinities of interaction. A prediction from this hypothesis (see "Discussion") is that the binding of E1 should increase when E1 is provided with a full set of interacting ligands, *i.e.* we might be able to detect E1 interactions with intact laminin that possesses all three short arms. Using the ultracentrifugation assay, binding of intact laminin to E1 was compared to E1′ in the presence of calcium (Fig. 6, *upper panel*). A shift of about one-third of that measured with E1′ was observed, and therefore, laminin-E1 binding, while measurable, was reduced compared to the larger E1′ fragment. Consistent with this observation was the finding that when labeled E1 was passed down a Sepharose CL-2B column in the presence of an equimolar concentration of

terminal globule on the B2 arm. Cathepsin G fragment C1–4 (*f*) is the largest complex and contains all three short arms with their respective globules. Fragment P1′ (*g*), like E1′ and E1, has the same asymmetrical shape (arms are ~46, ~32, and ~21 nm long, respectively) without any globules. Images are shown contrast-reversed in groups and individually.

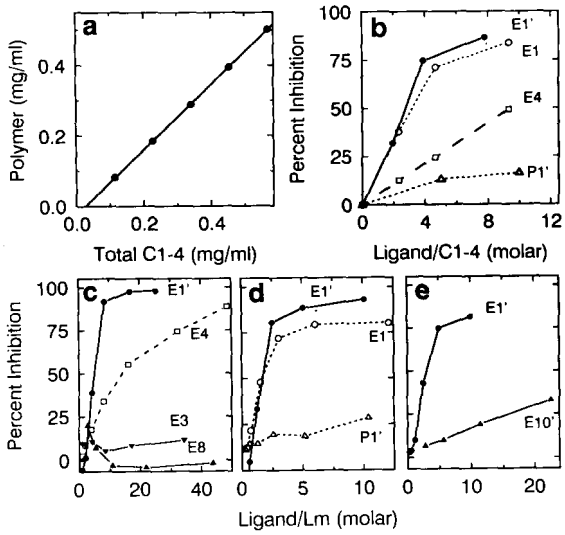

FIG. 3. **Polymerization of C1–4.** *a*, fragment C1–4 was dialyzed in the cold into assembly buffer (TBS containing 1 mM $CaCl_2$), diluted to various concentrations, and incubated at 37 °C for 2 h. Aliquots were then centrifuged, and the protein polymer was sedimented (10,500 rpm) and quantitated. Sedimented protein increased linearly as a function of total protein concentration above a critical concentration of 30 μg/ml. *b*, inhibition of C1–4 polymerization. Radioiodinated C1–4 (0.25 mg/ml) was incubated with unlabeled laminin fragments at 37 °C for 2 h in TBS/Ca and then sedimented. The short arm fragments E1′ (●), E1 (○), and E4 (□), unlike P1′ (△), inhibited polymerization. *c–e*, inhibition of laminin polymerization. Radioiodinated laminin (0.15 (*c*) and 0.25 (*d* and *e*) mg/ml) was incubated with laminin fragments in the same manner as described for C1–4. Fragments E1′ (●), E1 (○), and E4 (□) inhibited laminin polymerization, while fragments E3 (▼) and E8 (▲) had no effect and fragments P1′ (△) and E10 (▲) had only a small degree of activity. These data provided evidence that polymerization depends upon short arm interactions and does not require the long arm.

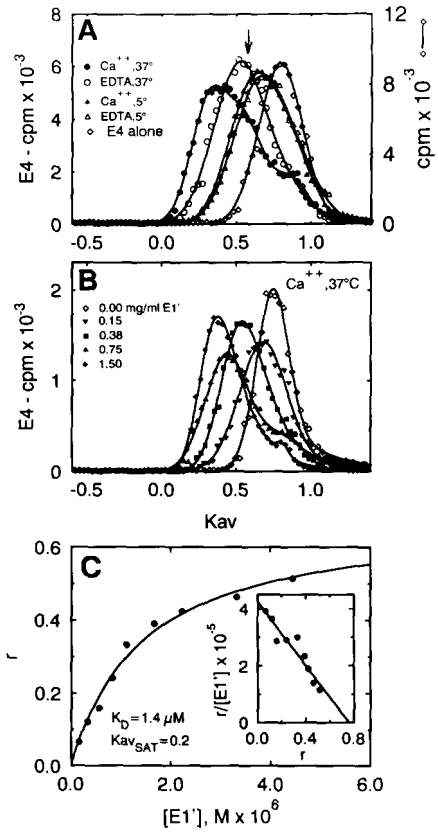

FIG. 4. **Equilibrium gel filtration assay of E1′-E4 binding.** A temperature-controlled Sepharose CL-2B column was equilibrated in TBS/Ca or TBS/EDTA containing various constant concentrations of E1′. A small (60 μl, 2.6 μg/ml) aliquot of radiolabeled E4 was applied to the gel filtration column as a narrow band, and fractions were collected. Binding resulted in the labeled fragment eluting as a larger species. *A*, effect of temperature and calcium on binding. E4 was passed down the column at 2 mg/ml E1′ in 1 mM calcium at 37 °C (●) and 5 °C (▲) or in 5 mM EDTA at 37 °C (○) and 5 °C (△). The earliest elution, and hence strongest binding, was measured in 1 mM calcium at 37 °C. Binding between the fragments was calcium- and temperature-dependent since chelation with EDTA led to a partial increase in elution volume and lowering the temperature led to a substantial increase in elution volume. The *arrow* indicates the nonbinding K_{av} for E1′. *B*, concentration dependence (E1′) of binding at 37 °C in the presence of 1 mM calcium. E4 eluted at earlier K_{av} values as a function of increasing E1′ concentration. ◇, no E1′; ▼, 0.15 mg/ml E1′; ■, 0.38 mg/ml E1′; ▲, 0.75 mg/ml E1′; ♦, 1.5 mg/ml E1′. *C*, determination of dissociation constant for E1′-E4 binding using a large number of determinations. As described in text, binding was measured from the known concentration of E1′ and an elution coefficient *r*, which is calculated from the binding K_{av} and the nonbinding K_{av}. The direct binding plot and Scatchard transformation (*inset*) are shown.

E1′ and E4 (4 μM each), E1 eluted 0.13 K_{av} unit higher than the nonbinding K_{av} (plot not shown).

Calcium Binding—Given a calcium-dependent interaction between short arm domains of laminin, we wanted to locate the calcium-binding region that modulated this interaction. Laminin, laminin/entactin, entactin, and fragments were evaluated for calcium binding using a $^{45}Ca^{2+}$ dot blot assay in which the protein concentration was varied (Fig. 7). Substantial label bound to laminin/entactin, laminin, entactin, and fragment E1′. A small degree of binding was detected for E8. However, little or no binding was detected for E1, P1′, E4, or E3. A total laminin digest bound to calcium as well as to intact laminin, making it unlikely that a major calcium-binding site was lost through proteolysis. We concluded that the principle calcium-binding sites are located in E1′ and entactin.

Calcium binding was also evaluated in a Western blot in which proteins were separated by SDS-PAGE and incubated with radiolabeled calcium after transfer of the protein bands to the nitrocellulose (Fig. 8). Reduced samples of laminin and laminin/entactin revealed that only the B chains of laminin and entactin bound to calcium, confirming published experiments (Chakravarti *et al.*, 1990). For fragments electrophoresed under nonreducing conditions, only fragment E1′ and entactin were observed to bind to calcium. Fragment E1′ possesses a major band migrating similar to the A chain of laminin and minor staining bands at ~90 and 40 kDa. Both the large band and the ~90-kDa band reacted with calcium. While the former is of laminin origin, the latter derives from entactin. We considered, but thought unlikely, the possibility that irreversible denaturation with loss of significant calcium binding may have occurred during SDS-PAGE. In the case of nonreduced samples, we note that the electrophoretic blots are in complete agreement with the dot blots (in which the samples were not treated with SDS) and that both are in agreement with equilibrium $^{45}Ca^{2+}$ dialysis carried out with native laminin/entactin, E1′, and E8 (Paulsson, 1988). Of the three proteins evaluated under equilibrium conditions (Paulsson, 1988), laminin/entactin was found to bind the strongest, E1′ to bind at an intermediate level, and E8 the weakest. Our finding the same relationship for the above proteins provided validation of the dot blot and transfer methods and permitted us to extend the study to the other fragments. The observations that calcium binds the B chain(s), but not the A chain;

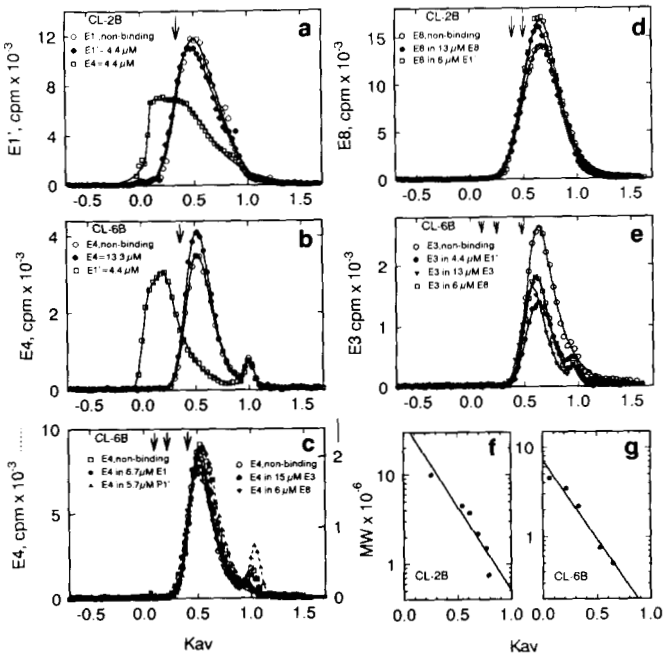

FIG. 5. **Equilibrium gel filtration of other fragment combinations.** Radioiodinated ligands were eluted from either Sepharose CL-2B or CL-6B in the presence of different protein components in assembly buffer at 37 °C. *a*, radioiodinated E1′ was eluted from a Sepharose CL-2B column in the absence of other laminin fragments (nonbinding) (○) or from the column equilibrated with 2 mg/ml (4.4 μM) E1′ (●). The position of an E1′ dimer was predicted by column calibration and is indicated with an *arrow*. E1′ eluted at a slightly lower K_{av} value in constant E1′, reflecting a very weak interaction. This small shift was reproducible. In contrast, E1′ eluted with a substantially lower K_{av} (~0.2) in the presence of 4.4 μM E4 (□). *b*, E4 was eluted from a Sepharose CL-6B column without other laminin components (5.6 μg) (○) or from the column equilibrated with 1 mg/ml (13.3 μM) E4 (●). The predicted K_{av} of an E4 homodimer is indicated with an *arrow*. No shift of labeled E4 was observed in constant E4. In contrast, a substantial shift was observed in the presence of 4.4 μM E1′ (□). Therefore, the only significant short arm interactions were between B1 and A and/or B2, but not between B1 and B1 or between A-B2 and A-B2 (in the absence of B1). *c*, radiolabeled E4 elution (nonbinding elution) (□, ○) was evaluated for short arm (- - -) and long arm (——) fragments as follows: 6.7 μM E1 (■- - -■), 5.7 μM P1′ (▲- - -▲), 15 μM E3 (●——●), and 6 μM E8 (▼——▼). The predicted K_{av} values for an E1′-E4 heterodimer, an E4-E8 heterodimer, and an E4-E3 heterodimer are indicated with *arrows*, from left to right. No shifts were detected other than a small shift in the presence of E8 (estimated 32 μM). *d*, the Sepharose CL-2B elution of radioiodinated long arm fragment E8 was evaluated in the absence of other laminin components (○) or in the presence of either 13 μM E8 (●) or 6 μM E1′ (□). No elution shift was detected. The predicted K_{av} values for an E1′-E8 heterodimer (*left arrow*) and an E8 homodimer (*right arrow*) are indicated. *e*, the Sepharose CL-6B elution of E3 was evaluated alone (nonbinding elution) (○) in comparison to 4.4 μM E1′ (●), 13 μM E3 (▼), and 6 μM E8 (□). The predicted K_{av} values for an E1′-E3 heterodimer, E3-E8 heterodimer, and E3 homodimer are indicated with *arrows*, from left to right. A shift to half-saturation was observed for E3 in E3 (~13 μM), and a small shift for E3 in E8 (~94 μM) and no shift for E3 in E1′ were detected. *f*, shown is the calibration of the Sepharose CL-2B column with laminin and laminin fragment (E1′, P1′, E8, E4, and E3) standards. *g*, shown is the calibration of the Sepharose CL-6B column with laminin fragment standards.

that calcium binds E1′, but not P1′; and that calcium does not bind to E4, E10, or (to any great extent) the long arm fragments were interpreted as evidence that the principal calcium-laminin binding requires globular domains of the B2 chain. However, since the A and B chains of laminin were separated by SDS-PAGE under *reducing* conditions before binding, it is possible that there exists a calcium-binding site in the native A chain that, unlike that found in the B chain, requires undisturbed disulfides for activity. An argument against this possibility is that E1, which possesses A chain globules in many of the molecules, but lacks the B2 outer globule, did not bind calcium under nondenaturing and nonreducing conditions. The difference in E1′ and E1 binding further suggested that a site is located in or near the outer (domain VI) globule of the B2 chain.

Summary of Fragment Interactions—A summary of the interactions measured by equilibrium gel filtration, the relative calcium binding affinities, and the degree to which fragments inhibit laminin polymerization is shown in Table II. The strongest fragment-fragment binding, by manyfold, was that observed between E4 and E1′, two of the three fragments that inhibited polymerization of laminin or C1–4. Calcium binding was found to reside principally in E1′. Fragment E1 inhibited polymerization and interacted to a lesser degree with intact laminin. However, an isolated interaction with E4 was not detected. This is consistent with a model in which three ligands are required for a detectable binding interaction and in which E1 possesses one out of the two E4-interacting binding sites present in E1′. Since E1 lacks the B2 outer globule, this is likely to be the second site.

Electron Microscopy of Short Arm Interactions—The inability to date to cleave E1′ into separate A and B2 arms, each possessing terminal globules, prevented the separate biochemical evaluation of the contribution of these two arms to polymerization. To circumvent this problem, we examined fragment complexes by electron microscopy (Figs. 9–11). First, we evaluated E4 incubated with E1′ (TBS/Ca, 37 °C) and compared this to E1′ and E4, each incubated separately under the same buffer and temperature conditions (Fig. 9). In the fragment mixture, we identified dimeric, trimeric, tetrameric, and larger linear oligomeric forms of E1′, sometimes visibly associated with E4, as well as monomers of each. In contrast, when E1′ was incubated alone, there was a substantial reduction of dimeric and larger forms (these relatively infrequent forms are not seen in the particular field shown). When E4 was incubated alone, nearly all molecules appeared to be monomeric, with rare head-to-head and head-to-tail associations seen. The molecular forms were counted and tabulated from a series of printed electron micrographs by direct inspection (Fig. 11). First, when E1′ was incubated with E4, 22% were dimeric and 16% were oligomeric with respect to E1′. In contrast, 7% were dimeric and <2% were oligomeric when E1′ was incubated alone, and 3% were dimeric and <1% were oligomeric when E4 was incubated alone. The electron microscopic findings were consistent with the fragment binding data using equilibrium gel filtration.

The population of complexes dimeric with respect to E1′ from the E1′/E4 incubation mixture was further examined (Fig. 10). Because of the asymmetrical shape of E1′, we found that it was possible to identify, in many cases, the arms that are involved in the formation of the complexes. Although there is some degree of heterogeneity in E1′, one could distinguish the longer A arm (~52 nm) from the shorter B2 arm (~35 nm) and from the rod-like B1 stub (~22 nm). The stub served to mark and to visually divide the two arms into the two unequal lengths. Other useful features in distinguishing the arms in complexes were that the stub formed either an acute angle or, less often, a right angle with the B2 arm; that about one of four B2 arms was associated with entactin (an intact dumbbell-shaped or globular fragment located near the junction of the inner globule and the inner rod-like domain); and that the inner globules of the A arm were often distin-

TABLE II

Interactions of laminin fragments

Shown below is a summary of the results from equilibrium gel filtration (Figs. 4 and 5 and plot not shown), calcium binding (Figs. 7 and 8), and laminin polymerization inhibition (Fig. 3) data. A semiquantitative scale (+++ to 0) was used to compare fragments with respect to calcium binding and inhibition of polymerization. When measuring binding between pairs of fragments, the smaller fragment was generally chromatographed as the labeled ligand for increased sensitivity. The largest nonbinding A-B2 short arm complex was used to determine interactions with other fragments.

Fragment 1	Fragment 2					Ca^{2+} binding	Inhibits polymer
	E4	E1′	E3	E8	E10′		
E4	No shift[a]	1.4 μM[b]	No shift	≥58 μM	≥76 μM[c]	0	++
E1′	1.4 μM	≥17 μM	No shift	≥65 μM	≥95 μM[c]	+++	+++
E1	≥190 μM	≥18 μM[c]	ND[d]	ND	ND	0	+++
P1′	No shift	ND	ND	ND	ND	0	0/+
E3	No shift	No shift	≥24 μM[e]	≥100 μM	≥120 μM[c]	0	0
E8	≥58 μM	≥65 μM	≥100 μM	≥65 μM	No shift[c]	+	0
E10/E10′	≥76 μM[c]	≥95 μM[c]	≥120 μM[c]	No shift[c]	No shift[c]	0	0/+

[a] No shift indicates that no interaction was detected by equilibrium gel filtration.

[b] K_D was determined by Scatchard analysis. All other constants estimated from K_{av} shift at one permeating protein concentration as described in text.

[c] Plot not shown.

[d] Not determined.

[e] The weak interaction appears to be mediated by labile disulfides (no shift is observed in the presence of 1 mM *N*-ethylmaleimide) and is not observed with the intact laminin G domain (Yurchenco *et al.*, 1993).

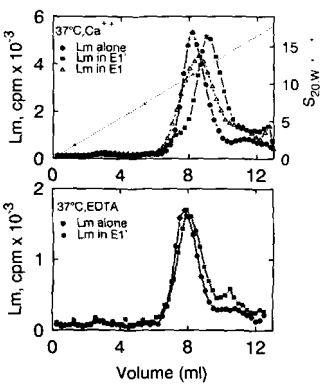

FIG. 6. **Equilibrium zonal velocity ultracentrifugation.** *Upper panel*, laminin (*Lm*) (radioiodinated) sedimented (40,000 rpm, 8 h, 5–20% sucrose gradients) in the absence of other protein (●) and in initially constant 3.3 μM E1′ (■) or E1 (△) in 1 mM calcium at 37 °C. Cytochrome *c*, aldolase, and catalase standards were sedimented in parallel (▲- - -▲). *Lower panel*, radioiodinated laminin alone (●) or in the presence of 3.3 μM E1′ (■) in 5 mM EDTA at 37 °C. Laminin binding to E1′ was strongly calcium-dependent. A weaker interaction with E1 was observed.

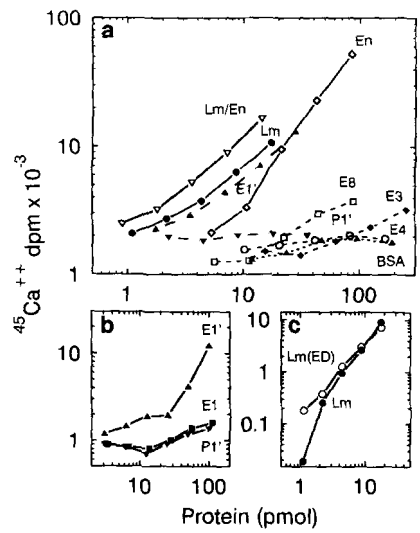

FIG. 7. **Calcium dot blot binding assay.** Laminin, laminin-entactin (*Lm/En*) complex, entactin (*En*), and fragments of laminin were serially diluted onto nitrocellulose. The membrane was then incubated with $^{45}CaCl_2$ (1 μCi/ml), and bound radioactivity was determined after washing the nitrocellulose. *a–c* represent three separate experiments. ▽, laminin/entactin; ●, laminin; ◇, entactin; ▲, E1′; □, E8; ▼, P1′; ■, E1; ♦, E3; ○, E4 (*a*) or laminin elastase digest mixture (*ED*; *c*). Both laminin and entactin were found to bind calcium. Of the fragments, E1′ possessed the highest level of activity, with a much lower level in E8 and little or no binding activity in E1, P1′, E4, and E3. Cleavage with elastase produced little or no loss of calcium binding activity.

guished. Fragment E4 (appearing typically as a ball with a short flexible tail) could also often be identified in E1′-E4 complexes. Most of the complexes whose arm orientations could be sorted out were found to consist of an A arm contacting a B2 arm, with or without an E4 visible at the junction (18 examples are shown in Fig. 10). The alternative orientations of A to A, B2 to B2, and stub to either A or B2 were much less frequent. The population of E1′ dimers (n = 126) identified in Fig. 11 (*upper panel*) was sorted out, by visual inspection of the micrographs, into types of arm interactions. First, nearly half (44%) were considered to be of ambiguous orientation. In some cases, the stubs could not be identified, and in others, the complexes were tangled or otherwise unresolvable. Of the remaining population, 43% were found to consist of the A chain contacting a neighboring B2 chain, 6% were between A chains, 3% were between B2 chains, and 3% involved the stub. E4 molecules could be observed contacting the A-B2 junction in a significant number of cases (43%), and examples are shown. Failure to recognize the small attached E4 may occur because of orientation or because it does not project from the arms of the large E1′ dimer. Alternatively, some of the E4 molecules may have dissociated from E1′. However, given that formation of these complexes required E4 (as demonstrated both biochemically and in electron micrographs), we inferred that essentially all of the E1′-E1′ complexes bind to E4 in the form of a heterotrimer and concluded that the principal interactions in the formation of E1′-E4 complexes are mediated between the peripheral regions of all three short arms.

DISCUSSION

Laminin polymeric networks, formed through relatively low affinity interactions, have been found to make a major contribution to basement-membrane architecture (Yurchenco *et*

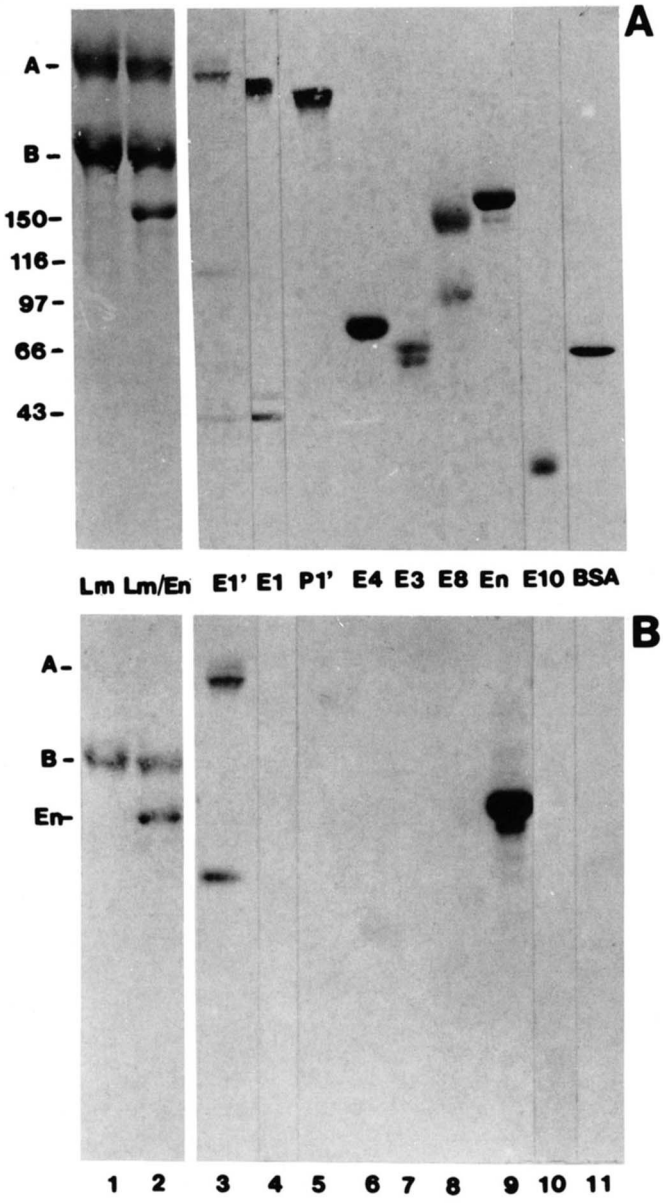

FIG. 8. **Calcium binding to electrophoretically transferred fragments.** Proteins were electrophoresed on 3.5–12% slab gels under reducing (*lanes 1* and *2*) or nonreducing (*lanes 3–11*) conditions and then electrophoretically transferred onto nitrocellulose. *A*, Amido Black stain of nitrocellulose prepared after autoradiography; *B*, autoradiograph of nitrocellulose. The samples from *lanes 1–11* were laminin, laminin-entactin complex, E1′, E1, P1′, E4, E3, E8, entactin, E10, and bovine serum albumin. The reduced B chain and entactin (*En*), but not the A chain, reacted with calcium. Furthermore, the high molecular mass A-B2 band of E1′ as well as a ~100-kDa band of E1′ (an entactin/nidogen-derived fragment) bound to calcium.

al., 1992). In this study, we addressed the question of which domains or regions of laminin are involved in this polymerization process.

Short Arm Interactions—Using assay systems that permitted evaluation and quantitation of dissociable interactions between laminin fragments representing most of the laminin molecule, we localized the principal binding as that occurring between the short arm fragments E4 and E1′, two fragments found also to inhibit polymerization. Because significant binding was not observed between E4 and P1′ (the latter lacking the globular domains and having little inhibition activity) or between E10′ (localized to the inner globule of the B1 chain short arm) and any fragment, we concluded that the interactions require sites present in B1 chain peripheral domains VI and/or V and the globular regions of the other short arms. Although fragment E1′ possesses a moiety of entactin (nidogen), it is unlikely that entactin provides a polymer-binding site. First, laminin free of entactin polymerized in an identical manner as the laminin-entactin complex (Yurchenco *et al.*, 1992). Second, entactin (nidogen) expressed in mammalian cells had no laminin polymerization inhibition activity (using recombinant protein provided by Drs. Ulrike Mayer and Rupert Timpl (Max-Planck-Institute)).[3] More precise localization of interacting domains with respect to the relative contributions of the A and B2 short arms was provided by visualization of replicas of the mixed fragments by electron microscopy. Mixtures of E4 and E1′ incubated together developed the largest fraction of complexes with dimers, trimers, tetramers, and even larger linear oligomers. We focused on the structure of dimeric E1′ because it had the simplest morphology and was the easiest to analyze. Most of the identifiable complexes were connected by the A short arm of one E1′ to the B2 short arm of the other, with a significant fraction possessing an observable E4 (B1 domains VI and V) at the juncture. This in turn strongly suggested that the laminin polymer is formed by the union of each of three different short arms (A, B1, and B2) for each bond (Fig. 12*a*).

The E1′-E4 dissociation constant measured under equilibrium conditions was 1.4 μM, weaker than the critical concentration for polymerization (0.1 μM), which is likely to equal the dissociation constant for the propagation step of polymerization (Oosawa and Asakura, 1975). This difference is likely due to the number of bonds formed upon the addition of each monomer to a growing polymer, *i.e.* in the case of fragments, only one triple interaction is formed by the addition of each E1′-E4 pair, whereas in the case of intact laminin, each laminin has the ability to bind at three sites upon addition to a growing polymer. One mechanism that could produce the above binding would be one in which the terminal globule of each arm possesses two binding loci, *i.e.* site a in B1 binds to site a′ in A, site b in B1 binds to site b′ in B2, and site c in A binds to site c′ in B2. In this manner, only a single bond would be formed between any pair of arms, but a stronger *pair* of bonds would exist for each arm when all three arms associated with each other. The E1 data are consistent with such a mechanism. We believe that E1 inhibited laminin and C1–4 polymerization because its single ligand was sufficient to compete with and disrupt three-arm bonds present in the large polymer, while interactions between the single active arms in E1 and E4 would be extremely weak and difficult to measure. E1 interactions, on the other hand, would be detected with trivalent laminin or in E1′/E4 mixtures as observed.

Long Arm Role—The long arm globule has been found to support cell interactions mediated by a variety of integrins and other cell-surface binding proteins (reviewed by Mecham (1991)) and the binding of heparin/heparan sulfates (Yurchenco *et al.*, 1990, 1993). Previously, we observed complexes of laminin whose contacts were mediated by the ends of their long arms (Yurchenco *et al.*, 1985). The significance of these complexes for the active process of polymerization could not be determined by microscopy alone. The observations that the triple short arm complex C1–4 (which lacks the long arm) polymerized and that the two long arm fragments E8 and E3 both failed to inhibit polymerization of laminin indicated that the long arms did not participate in the central process of polymerization. This negative finding is in agreement with the conclusions of Beck *et al.* (1990). Furthermore, the obser-

[3] P. D. Yurchenco and Y.-S. Cheng, unpublished data.

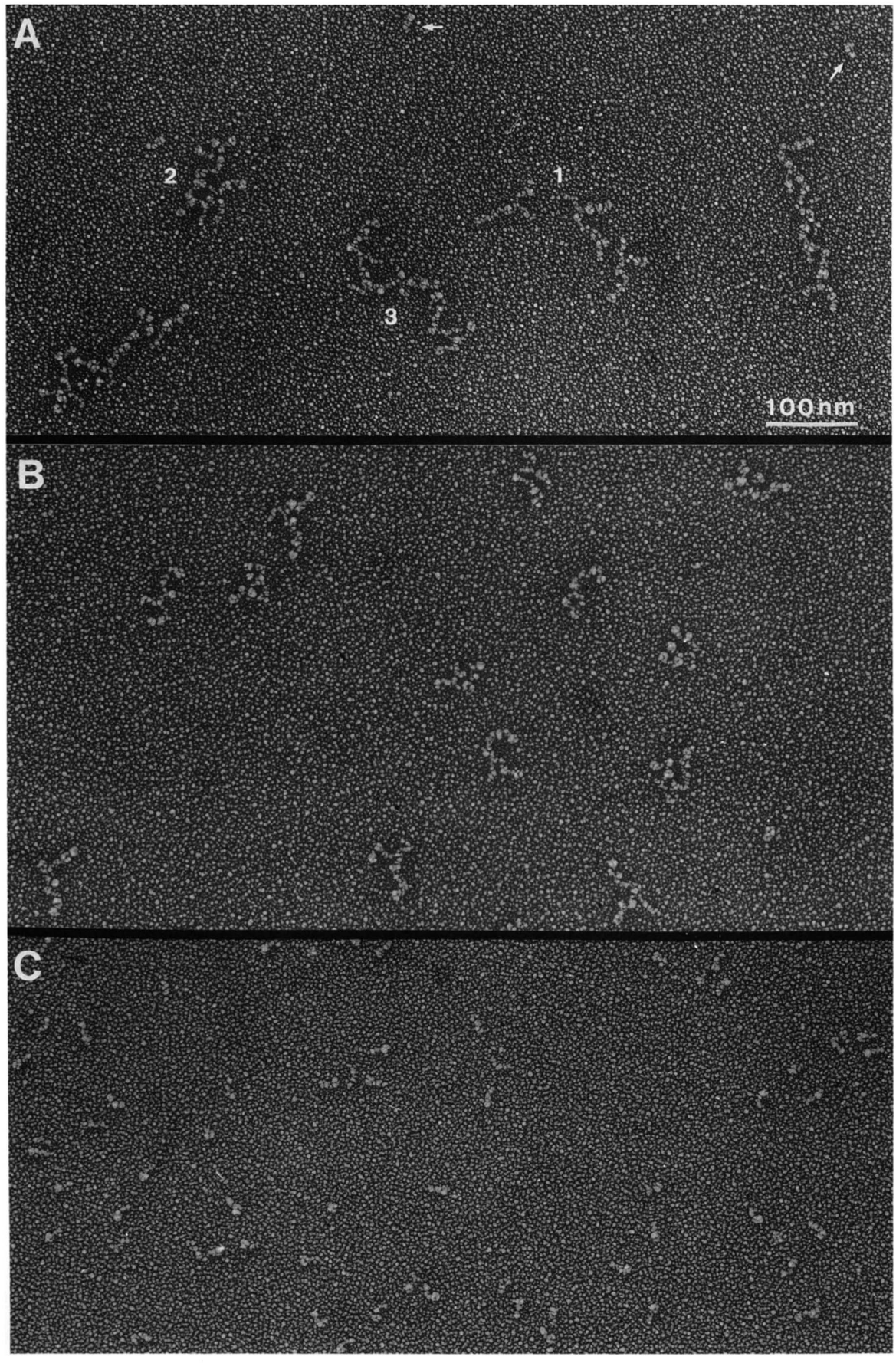

FIG. 9. **Electron microscopy of incubated fragments.** Fragments E1′ and E4 (each initially 4.4 μM) were incubated together (*A*) or alone (*B* and *C*, respectively) in TBS containing 1 mM calcium at 37 °C for 30–60 min and immediately prepared for rotary shadowing. Electron micrographs revealed that a large fraction of the E1′/E4 mixture contained dimeric and (mostly) linear oligomeric aggregates of E1′. The number of E1′ monomers observed in several complexes is indicated. *Arrows* identify free E4 molecules. Complexes larger than monomer were infrequently observed when each fragment was incubated alone.

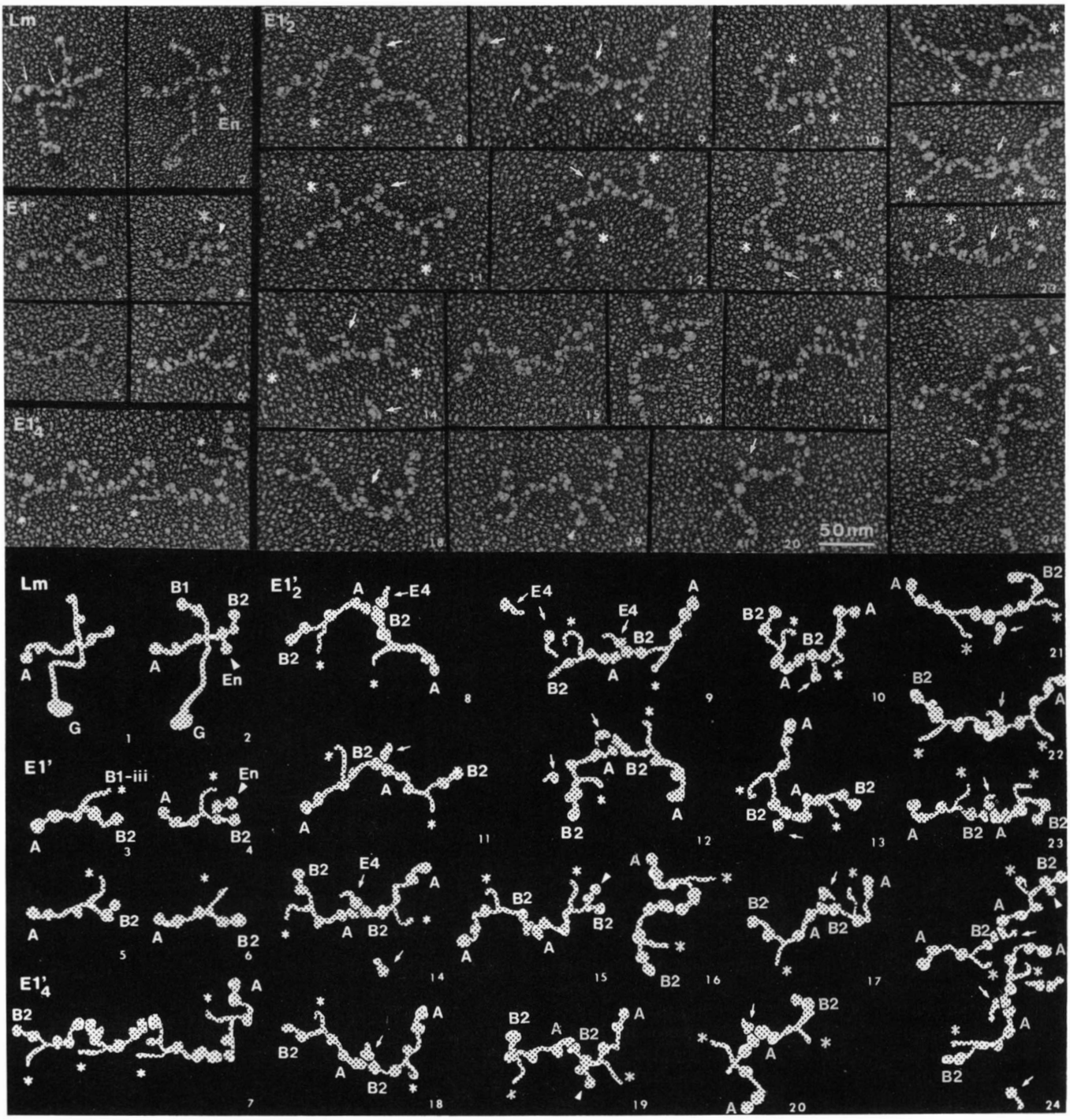

FIG. 10. **Electron microscopy of small E1′ complexes formed in presence of E4.** Gallery of selected images includes laminin (*Lm; top left*) with short A arm globules marked with *thin arrows*, laminin-entactin complex (entactin (*En*) indicated with *arrowhead*), and E1′ monomers as morphological standards. E1′ dimers formed in the presence of E4 were often associated at their junctions with an identifiable E4 fragment (examples marked with *arrows*). Because the A short arm is longer than the B2 short arm and their junctures were identified by the B1 stub (B1 domain III) (*asterisks*) as well as other morphologic markers, the A chain could be distinguished from the B2 chain in many examples. Nearly all oriented dimeric forms were in the form of an A arm contacting a B2 arm, with or without an obvious E4 (B1 chain) at the juncture. A linear tetramer ($E1'_4$) with the same arrangement is shown. Interpretations of the images, prepared from tracings of the micrographs, are shown below with the chain arrangements indicated.

vation that E8 or E3 bound weakly or not at all to any other fragment was interpreted as evidence that the long arm does not form supplemental (decorative) bonds in addition to those required for polymerization. The long arm-mediated dimers observed previously in electron micrographs therefore appear to represent a minor phenomenon unrelated to polymerization. However, the long arms may play a significant role in the alteration of polymerization in the presence of heparin (Yurchenco *et al.*, 1990) by virtue of the heparin-binding site present in G domain.

Calcium Binding and Laminin Polymerization—Calcium has been found to play a role both in the conformation of laminin (Paulsson *et al.*, 1988) and in laminin polymerization (Yurchenco *et al.*, 1985; Paulsson, 1988). The significance of

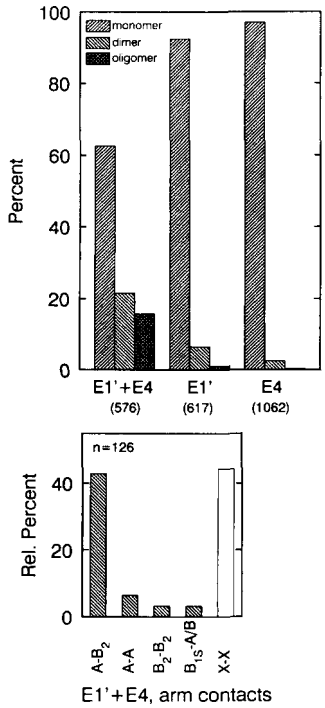

FIG. 11. **Distribution of molecular forms in electron micrographs.** Electron micrographs from the experiment described in Fig. 9 were scored with respect to oligomeric size (*upper panel*) and orientation (*lower panel*). *Upper panel*, molecular forms were counted by direct inspection (number of forms indicated in *parentheses*). A substantial increase in the fraction of dimeric and larger oligomeric forms was observed when E1′ was incubated with E4. *Lower panel*, dimeric E1′ population formed by incubating E1′ with E4 was further differentiated with respect to interacting arms. *B1S-A/B* indicates an observed contact between the B1 stub (B1 domain III) and any arm, and *X-X* indicates a dimer in which the arms involved in attachment could not be identified. Nearly all complexes with recognizable orientation involved A to B2 short arm interactions between E1′ molecules.

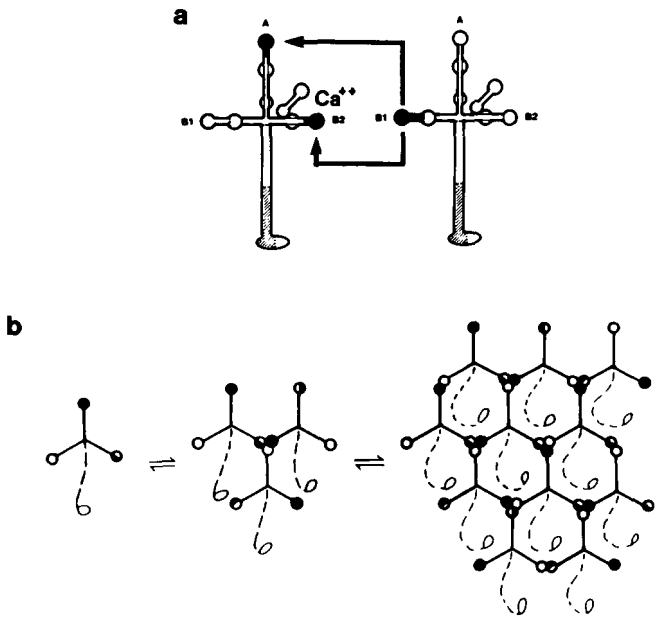

FIG. 12. **Three-arm interaction model.** *A*, from a biochemical and electron microscopic analysis of fragment interactions, it could be deduced that the principal bond(s) of polymerization were between B1 chain domains VI and/or V and the domain VI globules (with or without their immediately adjacent regions) of the A and B2 chains. Calcium binding was localized to the globular regions of E1′, most probably B2 domain VI alone (as well as to entactin, which is not required for polymerization). *B*, a model for polymerization consistent with the data is that the principal bond of polymerization is created by the joining of each of the three short arms. The primary bond is formed by terminal globule with or without the adjacent epidermal growth factor-like repeats. With such a polymerization, the free ends would be free to join their respective partners, forming a polymer with complete and equimolar consumption of free arms. The long arms would normally be free then to participate in cell and glycosaminoglycan interactions. A schematic model is shown in which the A short arm ends in a *solid circle*, the B1 short arm ends in an *open circle*, and the B2 short arm ends in a *half-filled circle*.

divalent cation for basement-membrane structure is illustrated by the observation that EDTA can extract substantial quantities of laminin from basement membranes under conditions that otherwise favor assembly (Yurchenco *et al.*, 1992). An earlier study with laminin/entactin, E1′, and E8 revealed that laminin/entactin bound some 16 calcium ions, but only one to a few with affinities likely to affect self-assembly. In another study (Chakravarti *et al.*, 1990), the B chain(s) and entactin (nidogen), but not the A chain, were found to bind calcium. We further characterized calcium binding using nitrocellulose binding assays and found that while laminin and entactin both bind calcium, only laminin fragment E1′, in contrast to the other fragments, exhibits substantial binding and that this binding likely lies in the globular region of the B2 chain. Taken in conjunction with the protein-protein binding data, it appears likely that calcium binding confers the correct conformation for favorable binding to the other short arms. The calcium binding to entactin/nidogen, on the other hand, is unlikely to play a major role in laminin polymerization since entactin/nidogen is not required for polymerization.

Three-arm Interaction Model—The data support a model in which the essential central bond of laminin polymerization is formed by the joining of an A short arm to both a B1 short arm and a B2 short arm (Fig. 12*b*).[4] The binding of calcium to the B2 short arm probably activates polymerization by providing a favorable laminin conformation. The repeating unit of such a polymer is a single laminin "trimer" containing one such bond. A single such trimer could serve as a nidus for the accretion of free laminin monomers into a planar array, each interacting in the same manner.

The three-arm interaction model further suggests that the more flexible long arm of each monomer would be free to interact with cells or heparin/heparan sulfates out of the plane of the polymer. Given that some cells preferentially recognize the ends of long arms, these arms would be free to interact with laterally diffusing receptors in a lipid bilayer. It has been reported that the critical concentration of laminin polymerization is lowered on pure phospholipid bilayers (Kalb and Engel, 1991). While biological membranes are not likely to have free and surface-exposed lipid, the data raise questions about a special role for laminin receptors in its polymerization. In particular, is it possible that laminin polymerization can be membrane receptor-facilitated? Given a three-arm interaction model, laminin, upon insertion into a secretory vesicle, might become tethered by a receptor (*e.g.* $\alpha_6\beta_1$ integrin or cell-surface proteoglycan (Aumailley *et al.*, 1990; Yurchenco *et al.*, 1990)), leaving the short arms in the correct plane to bind to each other upon activation with extracellular calcium. If such a mode of assembly can occur, it would be limited to the available number of receptors, and any additional laminin

[4] While each laminin monomer possesses the necessary three ligands for assembly, the arms cannot bind to each other within a single monomer because the arms are too rigid: such structures are not observed by electron microscopy.

(*e.g.* in thick basement membranes) would polymerize free of the cell surface.

In most basement membranes, laminin coexists with type IV collagen as a double polymer in which the two networks are probably enmeshed (Yurchenco *et al.*, 1992). Laminin and type IV collagen can in turn be connected and stabilized through bridging molecules such as entactin/nidogen (Aumailley *et al.*, 1989; Fox *et al.*, 1991). On the other hand, some basement membranes during embryogenesis (Kusche-Gulberg *et al.*, 1992) possess laminin, but lack type IV collagen. In these matrices, laminin may provide the only network. Given the reversibility of laminin polymerization, this network may be particularly suitable for rapid morphogenetic changes.

Many basement membranes possess laminins that contain genetic variants of one or even several chains. While little is known about the functional differences in such variants, one might expect those chains that possess globular structures similar to those of classical laminin to polymerize (*e.g.* merosin A and synaptic B1 (Ehrig *et al.*, 1990; Hunter *et al.*, 1989)). It has been proposed that laminin sometimes is composed only of a B1 and B2 chain (Edgar *et al.*, 1988). Such two-chain laminins or laminins that possess a truncated A chain or contain a B2 chain lacking the outer domain VI globule (Kallunki *et al.*, 1992) would be unlikely to polymerize by the model proposed in this study.

Acknowledgments—We thank Michael Ward and Holly Colognato Pyke for technical assistance and Dr. Jules O'Rear for helpful discussions and advice.

REFERENCES

Aumailley, M., Wiedemann, H., Mann, K., and Timpl, R. (1989) *Eur. J. Biochem.* **184,** 241–248

Aumailley, M., Timpl, R., and Sonnenberg, A. (1990) *Exp. Cell Res.* **188,** 55–60

Beck, K., Hunter, I., and Engel, J. (1990) *FASEB J.* **4,** 148–160

Bruch, M., Landwehr, R., and Engel, J. (1989) *Eur. J. Biochem.* **185,** 271–279

Cantor, C. R., and P. R. Shimmel (1980) *Biophysical Chemistry, Part III: The Behavior of Biological Macromolecules*, pp. 849–886, W. H. Freeman & Co., San Francisco

Chakravarti, S., Tam, M. F., and Chung, A. E. (1990) *J. Biol. Chem.* **265,** 10597–10603

Deutzmann, R., Huber, J., Schmetz, K. A., Oberbäumer, I., and Hartl, L. (1988) *Eur. J. Biochem.* **177,** 35–45

Edgar, D. R., Timpl, R., and Thoenen, H. (1988) *J. Cell Biol.* **106,** 1299–1306

Ehrig, K., Leivo, I., Argraves, W. S., Ruoslahti, E., and Engvall, E. (1990) *Proc. Natl. Acad. Sci. U. S. A.* **87,** 3264–3268

Engvall, E., Earwicker, D., Day, A., Muir, D., Manthorpe, M., and Paulsson, M. (1992) *Exp. Cell Res.* **198,** 115–123

Fox, J. W., Mayer, U., Nischt, R., Aumailley, M., Reinhardt, D., Wiedemann, H., Mann, K., Timpl, R., Krieg, T., Engel, J., and Chu, M.-L. (1991) *EMBO J.* **10,** 3137–3146

Fujiwara, S., Wiedemann, H., Timpl, R., Lustig, A., and Engel, J. (1984) *Eur. J. Biochem.* **143,** 145–157

Fujiwara, S., Shinkai, H., Deutzmann, R., Paulsson, M., and Timpl, R. (1988) *Biochem. J.* **252,** 453–461

Gerl, M., Mann, K., Aumailley, M., and Timpl, R. (1991) *Eur. J. Biochem.* **202,** 167–174

Horwitz, A., Duggan, K., Greggs, R., Decker, C., and Buck, C. (1985) *J. Cell Biol.* **101,** 2134–2144

Hummel, J. P., and Dryer, W. J. (1962) *Biochim. Biophys. Acta* **63,** 530–531

Hunter, D. D., Shah, V., Merlie, J. P., and Sanes, J. R. (1989) *Nature* **338,** 229–234

Kalb, E., and Engel, J. (1991) *J. Biol. Chem.* **266,** 19047–19052

Kallunki, P., Sainio, K., Eddy, R., Byers, M., Kallunki, T., Sariola, H., Beck, K., Hirvonen, H., Shows, T. B., and Tryggvason, K. (1992) *J. Cell Biol.* **119,** 679–693

Kusche-Gulberg, M., Garrison, K., MacKrell, A. J., Fessler, L. I., and Fessler, J. H. (1992) *EMBO J.* **11,** 4519–4527

Laemmli, U. K. (1970) *Nature* **227,** 680–685

Lee, M. K., and Lander, A. D. (1991) *Proc. Natl. Acad. Sci. U. S. A.* **88,** 2768–2772

Lim, W. A., Sauer, R. T., and Lander, A. D. (1991) *Methods Enzymol.* **208,** 196–210

Mann, K., Deutzmann, R., and Timpl, R. (1988) *Eur. J. Biochem.* **178,** 71–80

Maruyama, K., Mikawa, T., and Ebashi, E. (1984) *J. Biochem. (Tokyo)* **95,** 511–519

Mecham, R. P. (1991) *FASEB J.* **5,** 2538–2546

Oosawa, F., and Asakura, S. (1975) *Thermodynamics of the Polymerization of Protein*, p. 199, Academic Press, New York

Ott, U., Odermatt, E., Engel, J., Furthmayr, H., and Timpl, R. (1982) *Eur. J. Biochem.* **123,** 63–72

Palm, S. L., McCarthy, J. B., and Furcht, L. T. (1985) *Biochemistry* **24,** 7753–7760

Paulsson, M. (1988) *J. Biol. Chem.* **263,** 5424–5430

Paulsson, M., and Saladin, K. (1989) *J. Biol. Chem.* **264,** 18726–18732

Paulsson, M., Aumailley, M., Deutzmann, R., Timpl, R., Beck, K., and Engel, J. (1987) *Eur. J. Biochem.* **166,** 11–19

Paulsson, M., Saladin, K., and Landwehr, R. (1988) *Eur. J. Biochem.* **177,** 477–481

Sasaki, M., and Yamada, Y. (1987) *J. Biol. Chem.* **262,** 17111–17117

Sasaki, M., Kato, S., Kohno, K., Martin, G. R., and Yamada, Y. (1987) *Proc. Natl. Acad. Sci. U. S. A.* **84,** 935–939

Sasaki, M., Kleinman, H. K., Huber, H., Deutzmann, R., and Yamada, Y. (1988) *J. Biol. Chem.* **263,** 16536–16544

Schittny, J. C., and Yurchenco, P. D. (1990) *J. Cell Biol.* **110,** 825–832

Studier, F. W., Rosenberg, A. H., Dunn, J. J., and Dubendorff, J. W. (1990) *Methods Enzymol.* **185,** 60–89

Towbin, H., Staehelin, T., and Gordon, J. (1979) *Proc. Natl. Acad. Sci. U. S. A.* **76,** 4350–4354

Yurchenco, P. D., and Schittny, J. C. (1990) *FASEB J.* **4,** 1577–1590

Yurchenco, P. D., Tsilibary, E. C., Charonis, A. S., and Furthmayr, H. (1985) *J. Biol. Chem.* **260,** 7636–7644

Yurchenco, P. D., Cheng, Y.-S., and Schittny, J. C. (1990) *J. Biol. Chem.* **265,** 3981–3991

Yurchenco, P. D., Cheng, Y.-S., and Colognato, H. (1992) *J. Cell Biol.* **117,** 1119–1133

Yurchenco, P. D., Sung, U., Ward, M. D., Yamada, Y., and O'Rear, J. J. (1993) *J. Biol. Chem.* **268,** 8356–8365